

# Early root alterations after orthodontic force application studied by light and scanning electron microscopy

Maria Mavragani\*, Ole Christian Amundsen\*\*, Nils Jørgen Selliseth\*, Pongsri Brudvik\*\* and Knut Andreas Selvig\*

Departments of \*Dental Research and \*\*Orthodontics and Facial Orthopaedics, Faculty of Dentistry, University of Bergen, Norway

**SUMMARY** The purpose of the study was to characterize root surface alterations in orthodontically moved teeth. Thirty-six 40–50-day-old male Wistar rats were used. The maxillary right first molar was mesialized by means of a fixed appliance, exerting 50 g of force upon insertion. One, 2 and 4 days after force application the animals were sacrificed (nine animals per observation period) and block sections processed for analysis. Nine animals served as untreated controls. In total, 20 specimens were prepared for examination of the mesial aspect of the mesiobuccal root by scanning electron microscopy (SEM). The remaining specimens were processed for light microscopy.

Three morphologically distinct types of resorption defect were observed: isolated small lacunae, wide shallow resorption bays, and deep resorption lacunae. The area occupied by each resorption type varied significantly ( $P < 0.05$ ) with time. Isolated small lacunae were the earliest to be observed, sometimes found in continuity with wide shallow resorption bays. Mononucleated macrophage-like cells were associated with both resorption types. Deeper lacunae extending into the dentine were found at the 4 day observation period. These always occurred within shallow resorption bays and appeared to be created by multinucleated cells.

From the sequence of the different root surface defects and associated cell types observed during the development of orthodontically induced root resorption, it may be concluded that different cell types, with different resorptive potential but functionally interrelated, are involved in the successive phases of the process, and that each cell type leaves a characteristic resorption pattern on the root surface.

## Introduction

Orthodontic root resorption has been associated with local damage of the periodontal ligament (PDL) due to over-compression. Retardation and stagnation of the blood flow in such pressure zones lead to sterile necrosis of the soft tissues (Reitan, 1951; Reitan and Kvam, 1971; Rygh, 1972, 1973). The damaged tissue is subsequently removed by phagocytic cells such as macrophages, foreign body giant cells, and osteoclasts (Kvam, 1972; Rygh, 1974; Lindskog and Lilja, 1984).

During the remodelling process, root resorption may occur as a side-effect of the cellular activity associated with removal of the necrotic tissue (Kvam, 1973; Rygh, 1977). The initial access of resorptive cells to the root surface occurs in the immediate periphery of the necrotic zone. The cells involved in that phase are mononucleated, stain negatively to tartrate-resistant acid phosphatase (TRAP) indicative of non-osteoclastic lineage, and resemble macrophages or fibroblasts (Brudvik and Rygh, 1993a,b). Root resorption beneath the main necrotic zone takes place at a later phase, during which multinucleated TRAP-positive cells without ruffled borders both remove the bulk of necrotic PDL tissue and resorb the outer layer of adjacent root cementum.

Multinucleated TRAP-positive odontoclast-like cells with ruffled borders may be found in the deeper root resorption lacunae (Brudvik and Rygh, 1994a,b).

It is apparent that different cell types participate in different phases and at different sites of orthodontic root resorption. Because different cells have different resorptive potential, various resorption patterns are expected on the root surfaces. Available information about tissue reactions following tooth movement is primarily based on light microscope (LM) studies of sectioned tissues. Scanning electron microscopy (SEM) permits visualization of surface structures and is particularly valuable in recording the morphology of mineralized tissues (Boyde and Jones, 1968). This technique provides enhanced visual assessment of root surfaces, unattainable with histological models reconstructed from serial sections (Reitan, 1974). The purpose of exploring morphology is to learn about function, as the morphological image represents the visual expression of functional activity.

The aim of the present investigation was to examine alterations of the root surface during the initial phase after orthodontic force application by SEM and to relate the results with the image of the soft tissue/hard tissue interface obtained by LM.

## Materials and methods

### *Animals and experimental procedure*

The material comprised 36 40–50-day-old male Wistar rats (Mol:WIST Han) weighing  $196 \pm 10$  g. Nine rats served as untreated control animals. All animals were housed in polycarbonate cages and fed a standard pellet diet (801157W Expanded Pellets, Stepfield, Witham, Essex, UK) with tap water *ad libitum*. The experimental protocol was approved by the Regional Committee for Animal Research Ethics, University of Bergen, under the supervision of the Norwegian Experimental Animal Board.

In the experimental group the maxillary right first molar was moved mesially by means of a closed coil spring (Elgiloy spring, F-31  $0.008 \times 0.032$ , Rocky Mountain Orthodontics, Denver, Colorado, USA), ligated to the mesial aspect of the first molar and through the eyelet on an incisor band (Brudvik and Rygh, 1993a) (Figure 1). The force exerted at the time of insertion was 50 g. The weight of the animals was recorded on the day of appliance insertion and before death. The animals were anaesthetized with a subcutaneous injection of fentanyl (Dormicum; F. Hoffmann-La Roche & Co. AG, Basle, Switzerland)/fluanison midazolam (Hypnorm; Janssen Pharmaceutica, Beerse, Belgium) (0.15–0.2 ml/100 g body weight).

Specimens for histology were harvested from control (day 0) and experimental animals 1, 2, and 4 days after force application (nine rats per time period). Specimens from 20 animals (five from each day group) were processed for SEM examination. Corrosion casts were prepared to provide an image of vascular elements of

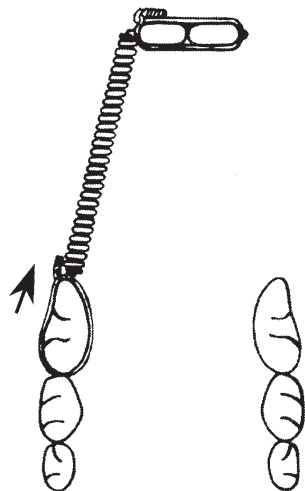


**Figure 1** Orthodontic appliance *in situ*: a closed coil spring ligated between an eyelet on the incisor band and the upper first molar, which is moved mesially. (Reprinted from Brudvik and Rygh, 1993a.)

the PDL to be presented separately. At the time of sacrifice each animal was administered 200 IU heparin/kg body weight and an overdose of anaesthesia subcutaneously. The external carotid arteries were exposed bilaterally, and polyethylene catheters inserted, permitting the jaws to be perfused with McDowell's fixative (Warshawsky and Moore, 1967) followed by liquid acrylic resin (Mercox cl RR, Vilene Hospital Inc., Tokyo, Japan). Following polymerization of the resin, the maxilla from each animal was dissected out and immersed in liquid nitrogen. The frozen maxilla was cut transversely with a stainless steel wheel (Komet 22  $\times$  0.15 mm, Lemgo, Germany), through the mesiobuccal root of the right first molar. Soft tissues were dissolved by maceration in 20 per cent NaOCl. The mesial part of the mesiobuccal root was removed, briefly dehydrated in graded ethanol baths, dried in air and finally mounted on aluminium stubs and coated with gold for examination in a SEM (SEM 515 Philips, Eindhoven, The Netherlands) at an acceleration voltage of 15 kV.

The remaining 16 animals (four from each day group) were processed for LM study. The animals were killed by an overdose of anaesthetic and were subsequently perfused through the left heart ventricle with McDowell's solution. Following dissection, the right half of the maxilla including the first, second, and third molars was kept in fixative for 24 hours at 4°C, rinsed in 0.1 M sodium cacodylate buffer containing 0.2 M sucrose, and decalcified in 0.25 M ethylene diamine tetraacetic acid (EDTA; 10 per cent) at 4°C for about 6 weeks. The specimens were then embedded in paraffin and parasagittal sections of the teeth were cut at 6  $\mu$ m. The area of investigation was the mesial aspect of the mesiobuccal root (Figure 2). Every fifth glass slide (five sections per slide) was stained with haematoxylin and eosin. The slide showing the greatest length of the mesiobuccal root and four adjacent slides covering 120–150  $\mu$ m in the buccolingual direction were studied by LM.

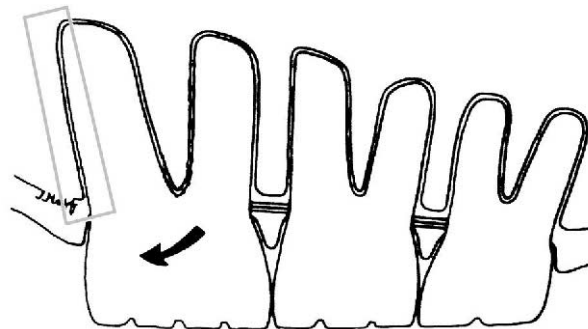


**Figure 2** A schematic illustration indicating the parasagittal section, the direction of tooth movement (arrow) and the area of investigation (box).

### SEM morphometrics

During SEM examination, sequential electron micrographs were taken from each specimen along the long axis of the root in a standardized manner. Four sequential electron micrographs at  $\times 406$  magnification were obtained at a right angle to the root surface, starting from the cemento enamel junction and covering an area of  $237.6 \times 10^3 \mu\text{m}^2$  of each root (Figure 3). The area occupied by each of three morphologically distinct types of lacuna (small isolated lacunae, superficial resorption bays, and deep lacunae extending to the dentine) was measured on the electron micrographs using an image analysis system (analySIS 2.1, Soft-Imaging Software GmbH, Münster, Germany). Additionally, the diameter of the small isolated lacunae was measured. The total area of each type of lacuna per tooth was then estimated.

### Statistical methods

The Kruskal–Wallis test was used to detect any overall significant difference between the four time groups, for each considered variable. In the case of a significant result ( $P \leq 0.05$ ), a Mann–Whitney test was performed to compare pairs of groups.

Twenty randomly selected sections were re-counted within a 3 month interval, in order to test for intra-examiner error. The normal distribution of the sample of the differences between the double measurements was initially tested by the Anderson–Darling normality test (Stephens, 1974). The systematic error between the double measurements was then evaluated using the paired *t*-test, and the measurement error by intraclass correlation coefficient. No significant systematic differences were found and the measurement error was considered acceptable.

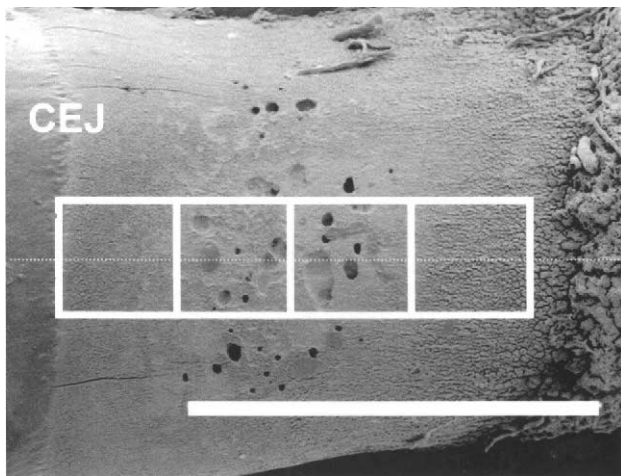


**Figure 3** A low power scanning electron micrograph illustrating the axial sequence of micrographs recorded from each specimen through the centre of the defect (bar = 1000  $\mu\text{m}$ ).

## Results

### Animals

The weight of the animals was only slightly reduced (approximately 10 g) during the first 2 days of the experiment and was normalized by day 4. The force introduced was active during the experimental period and gradually declined to approximately 58 per cent on day 4.

### SEM observations

*Types of lacuna.* SEM examination showed three morphologically distinct types of lacuna (Figure 4): (a) small isolated lacunae, (b) wide shallow resorption bays with no detectable dentinal tubules, and (c) deep resorption lacunae extending into the dentine.

The Kruskal–Wallis test revealed that the area occupied by each type of lacuna, as well as the diameter of the small isolated lacunae, varied significantly during the observation period (*P*-values for small isolated lacunae 0.025, their diameter 0.047, shallow lacunae 0.045, deep lacunae 0.05) (Figure 5). The Mann–Whitney tests showed significant differences with regard to the extent of shallow lacunae between days 0 and 1, 0 and 2, 0 and 4, as well as deep lacunae between days 0 and 4. The total area and the mean diameter of small isolated lacunae differed significantly between days 0 and 4, as well as between days 1 and 4 (Table 1).

*Control group.* The untreated animals showed a remarkable morphological variation in the root surface (Figure 6). Most of the control roots exhibited areas covered by undamaged cementum, with a characteristic mosaic-like surface pattern and mineralized projections. Small isolated lacunae were often seen scattered on their surface. Superficial resorption bays were not

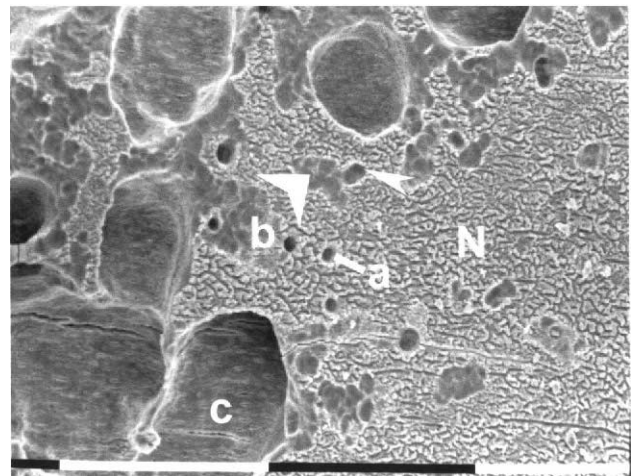


**Figure 4** Distinct types of lacuna on the root surface: small isolated (a), shallow (b) and deep (c). Small lacuna (small arrow) in continuity with superficial resorption bay (large arrow). N, normal cementum. Day 1, scanning electron microscope (bar = 100  $\mu\text{m}$ ).

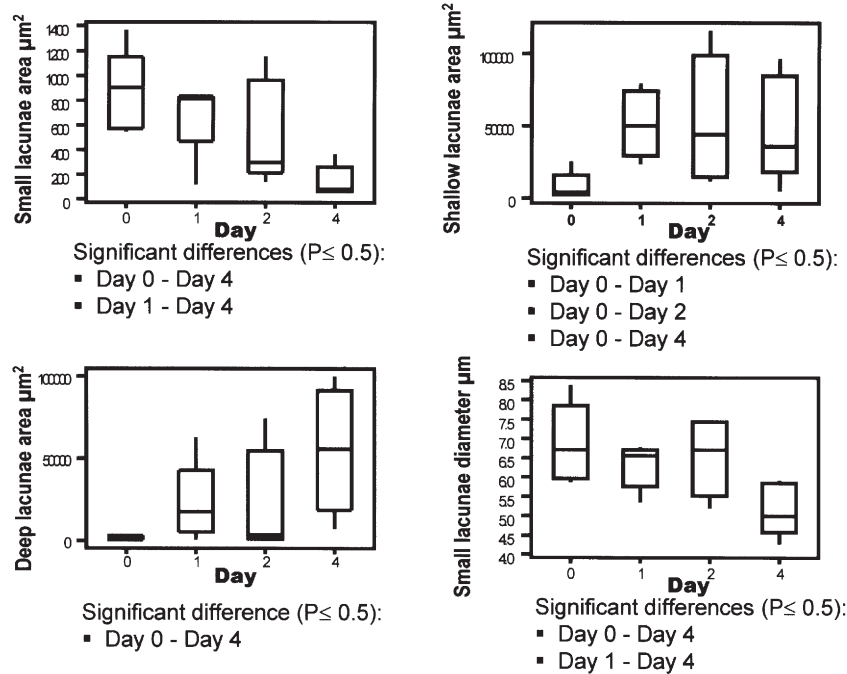


**Figure 5** Boxplots of the area of each lacuna type and small lacunae diameter according to time. The horizontal line inside each box indicates the median. The bottom of each box is at the first (Q1) and the top at the third (Q3) quartile. By default, the vertical lines (whiskers) extend from the top and bottom of the box to the adjacent values, the lowest and the highest observations still inside the region defined by the lower limit  $Q1 - 1.5(Q3 - Q1)$  and the upper limit  $Q1 + 1.5(Q3 - Q1)$ .

**Table 1** P-values from the Mann–Whitney test for pairs of day groups.

	Day 0–day 1	Day 0–day 2	Day 0–day 4	Day 1–day 2	Day 1–day 4	Day 2–day 4
Deep area	0.09	0.4	0.01	1.00	0.21	0.14
Shallow area	0.02	0.04	0.04	1.00	1.00	0.83
Small isolated area	0.40	0.21	0.01	0.53	0.04	0.09
Small isolated diameter	0.53	0.83	0.02	0.67	0.04	0.06

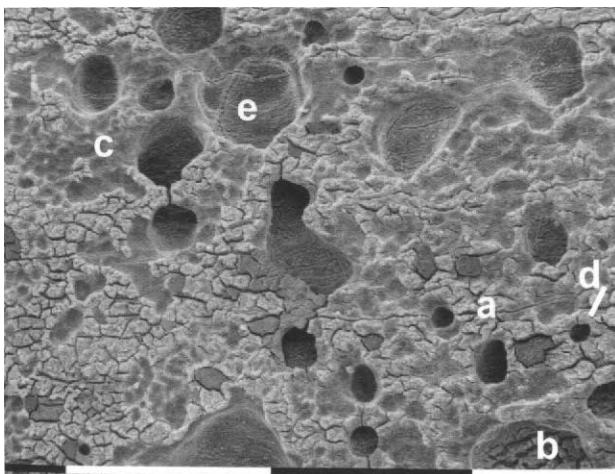


**Figure 6** The surface of a control root exhibiting intact cementum (a), repaired earlier resorption (b), superficial resorption (c), a small isolated lacuna (d), and deep resorption with open dentinal tubuli (e). Day 0, scanning electron microscopy (bar = 100  $\mu\text{m}$ ).

uncommon, whereas deep resorption lacunae involving the dentine were occasionally found. Some roots presented an uneven surface covered by cementum, indicative of repaired earlier resorption.

*Experimental group.* Small isolated lacunae in areas of healthy cementum were often observed at the beginning of the experimental period (Figure 7a), sometimes in continuity with shallow resorption bays (Figure 4). The area of root surface occupied by such defects was reduced during the experimental period. Their mean diameter also diminished; from 6.7  $\mu\text{m}$  on day 0 to 5.0  $\mu\text{m}$  on day 4. During the late stages, small isolated lacunae were mostly found along the periphery of the body of the defect.

The area of the shallow resorption bays was significantly higher on day 1 following force application compared with the control roots (Figure 7b). Areas of uneven surface morphology exhibited resorption into

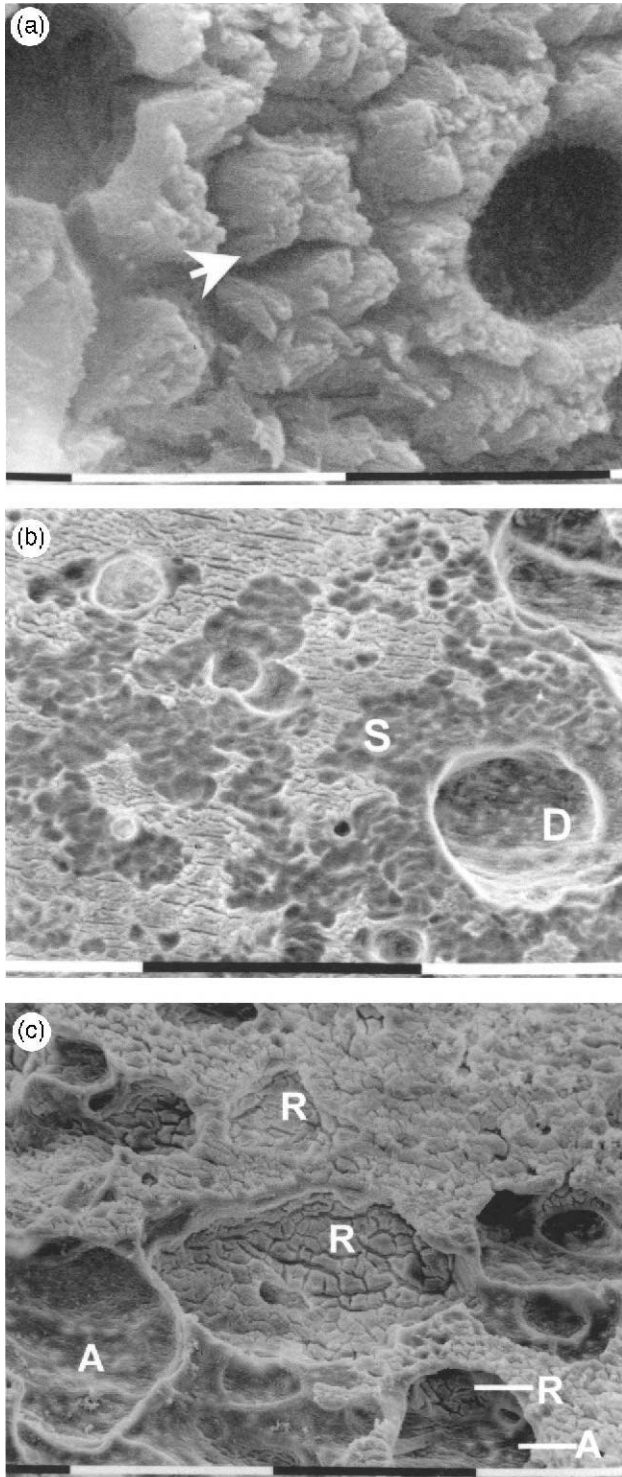


**Figure 7** (a) Small isolated lacunae in an area of healthy cementum. The arrow shows the mineralized part of Sharpey's fibres extending from the root surface. Day 1, scanning electron microscopy (SEM) (bar = 10 µm). (b) Deep resorption (D) with exposed dentinal tubuli in an area of superficial resorption lacunae (S). Day 1, SEM (bar = 100 µm). (c) Exposed dentinal tubuli indicating active resorption (A), in an area of repaired earlier resorption lacunae (R). Day 1, SEM (bar = 100 µm).

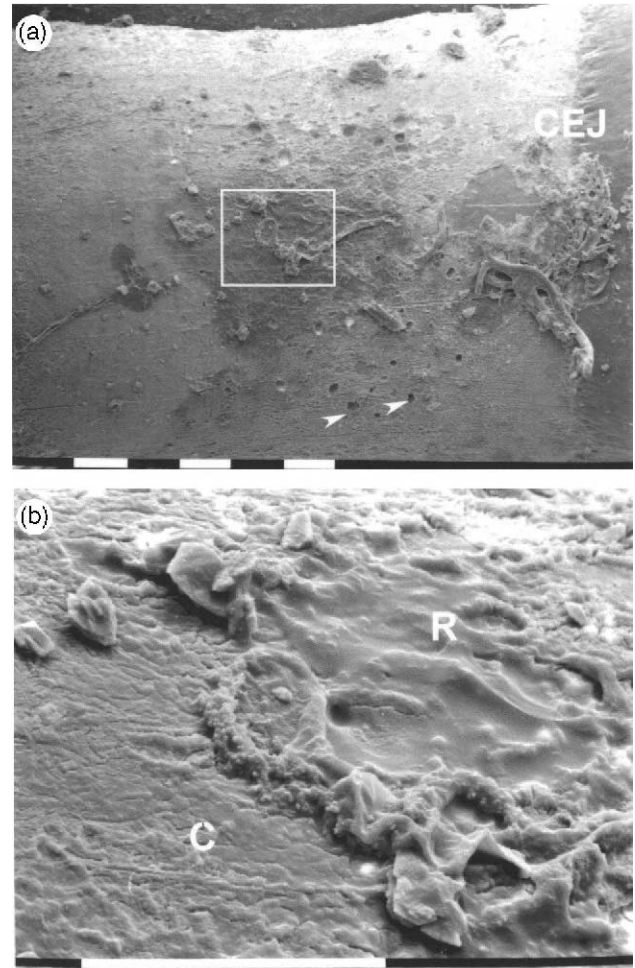


**Figure 8** (a) Tissue remnants on the root. Resorption at the periphery of the necrotic zone (small arrows). CEJ, cemento enamel junction. (b) Enlargement of the framed area in (a), showing the smooth appearance of the cementum (C) and remnants of necrotic tissue (R) on the root. Day 2, scanning electron microscopy (bar = 100 µm).

the dentine (Figure 7c). Tissue remnants were often observed on the root surface by the second day of the experiment (Figure 8a). Cementum in the vicinity of such areas had a smooth appearance, without mineralized projections (Figure 8b).

Deep resorption lacunae, with open dentinal tubuli (Figure 9a), were invariably located in fields of already existing shallow resorption bays (Figure 7b). In areas covered by healthy cementum, resorption occurred as an undermining process, leaving sharp edges at the periphery of the resorption bay (Figure 9b). Vascular elements were often observed in the vicinity of the deep resorption lacunae (Figure 9b, c).

*LM observations*

*Control group.* Observations under LM corresponded to the findings by SEM (Figure 10). Repaired resorption lacunae were noted in some control specimens. Small

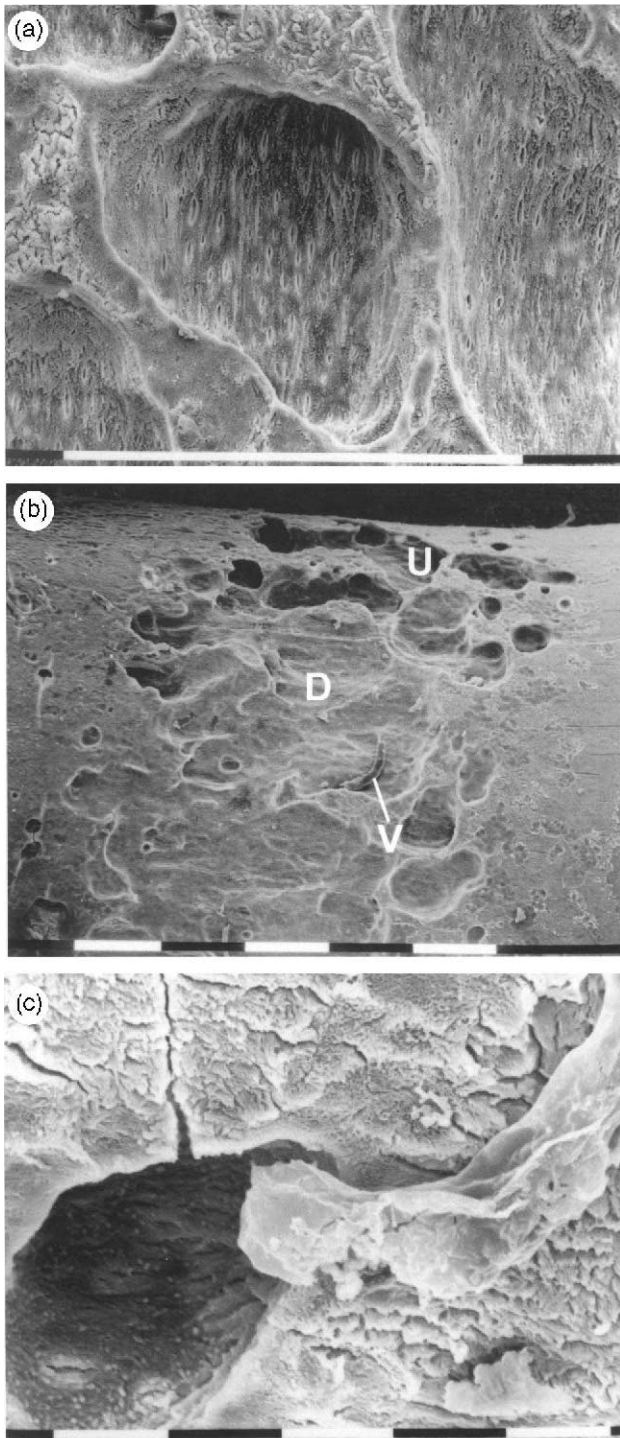


**Figure 9** (a) Deep resorption lacunae with uncovered dentinal tubuli. Day 4, scanning electron microscopy (SEM) (bar = 100  $\mu$ m). (b) Deep resorption lacunae with uncovered dentinal tubuli (D). Undermining resorption with sharp edges (U) shows the greater resistance of the cementum. Remnant of a vessel (V) in close relation to the resorption bay. Day 4, SEM (bar = 100  $\mu$ m). (c) Vascular remnant in close relation to a deep lacuna. Day 4, SEM (bar = 10  $\mu$ m).

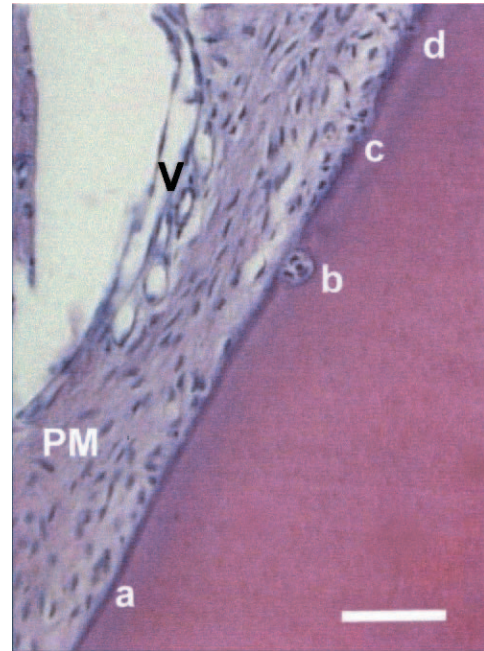


**Figure 10** Variation in an untreated root. Intact cementum (a), repaired resorption with cementum deposition (b), superficial resorption by mononucleated cells (c), a small isolated lacuna with a mononucleated cell (d). Vessel (V) in the periodontal membrane (PM). Day 0, light microscopy (bar = 50  $\mu$ m).

lacunae appeared as isolated cavities in the cementum and were occupied by mononucleated cells. Mononucleated cells were also seen related to more extensive but shallow bays that did not extend through the full thickness of the cementum.

*Experimental group.* The PDL in the pressure zone showed early signs of disorganization on day 1, evidenced by structureless spaces within the compressed PDL (Figures 11, 12a). Superficial cementum resorption was

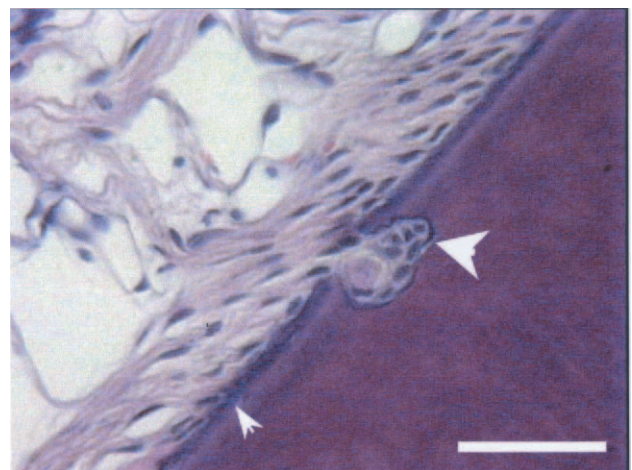


**Figure 11** Superficial resorption starts with elongated mononucleated cells lining up along the root (small arrow). An initial attack on the reparative cementum of an earlier repaired lacuna (large arrow). Day 1, light microscopy (bar = 50  $\mu$ m).

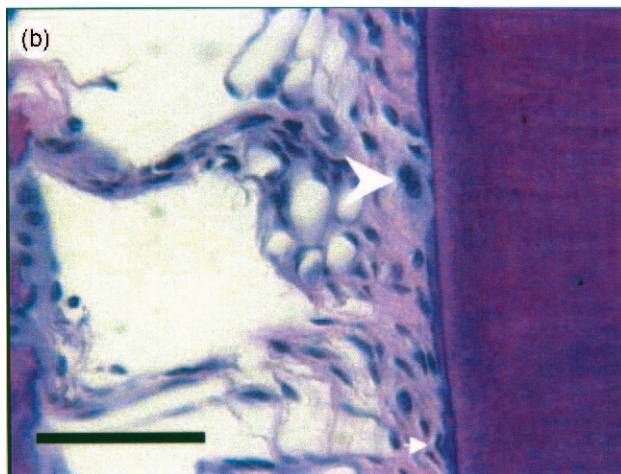
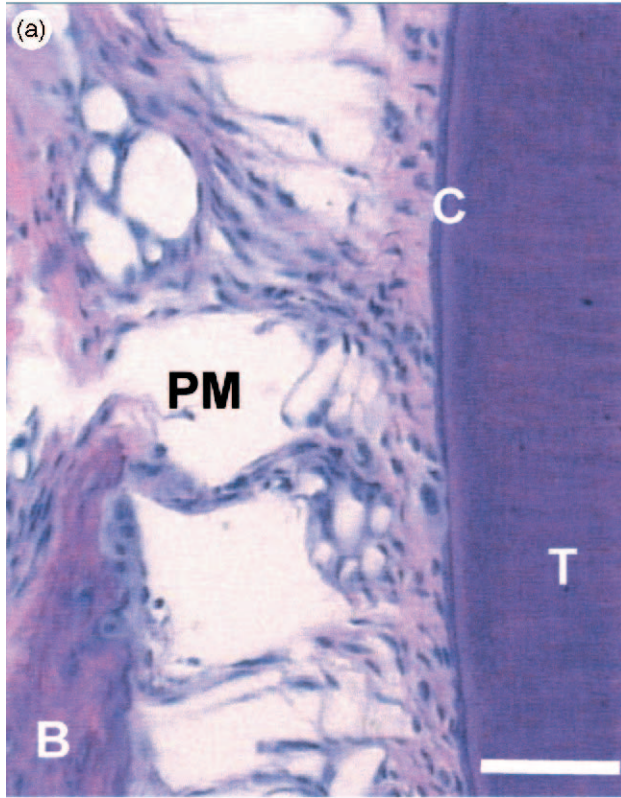


**Figure 12** (a) Cementum resorption by mononuclear cells under disrupted periodontal membrane (PM) at the pressure zone. B, bone; T, tooth; C, cementum. (b) Detail from (a): elongated flattened (small arrow) and larger (large arrow) mononucleated cells resorb cementum at different depths. Day 2, light microscopy (bar = 50  $\mu$ m).

a common finding, often seen associated with elongated mononucleated cells. Mononucleated macrophage-like cells with larger nuclei resorbing cementum at a greater depth were observed by day 2 (Figure 12b).

Deeper lacunae extending into the dentine were seen on day 4 following force application. They were often

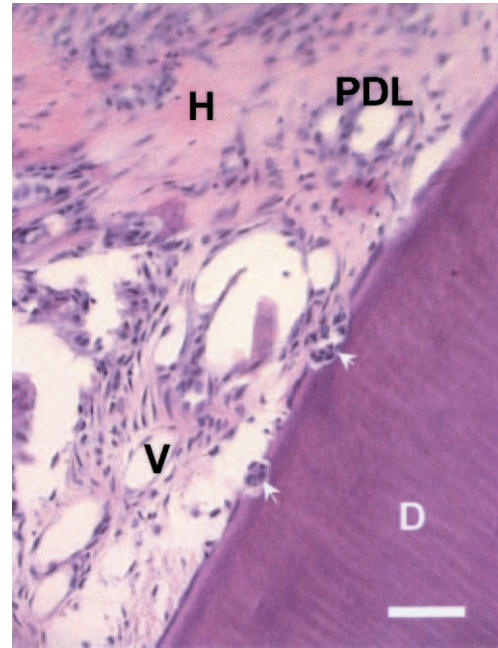


**Figure 13** Multinucleated clast cells (arrows) in deep resorption lacunae in an area of superficially resorbed cementum. Vessels (V) in close vicinity to the root surface, hyaline tissue (H), root dentine (D), periodontal ligament (PDL). Day 4, light microscopy (bar = 50  $\mu$ m).

occupied by multinucleated clast cells (Figure 13). Vascular elements were observed in their vicinity.

**Discussion**

*Method*

This study utilized both SEM and LM in order to record the surface area as well as the depth of root resorption defects following application of an orthodontic force. During specimen preparation for SEM the organic part was dissolved, allowing alterations of the mineral component of the root surface and the ‘footprints’ of cells on the mineralized tissue to be observed. The area of cratering on the root surface was evaluated as an indicator of cell activity. Although actual changes were three-dimensional, the measurement of surface area was considered satisfactory for comparison of data between the experimental subgroups. However, the third dimension was assessed by referring to defect depth as extending into the cementum only or into the dentine. LM provided an evaluation of the organic tissues and the identification of the cells related to different types of resorption lacuna. The standardized method of orthodontic force application permitted correlation of results obtained by the two histological techniques. Rather short observation periods were

selected based on previous studies of the initial phases of orthodontic tooth movement (Brudvik and Rygh, 1993b; Hellsing and Hammarström, 1996). The method of force application was identical to the one described by Brudvik and Rygh (1993a), using a force of 50 g, which has been considered optimal for provoking experimental root resorption.

#### *Control animals*

A striking finding was the variation in surface morphology of untreated roots. With SEM, undamaged cementum showed the characteristic mosaic-like pattern with deep grooves, presumably representing the cores of Sharpey's fibres (Lindskog, 1982). Often the calcified part of Sharpey's fibres was seen protruding from the root surface (Selvig, 1964; Boyde and Jones, 1968; Barber and Sims, 1981; Hellsing and Hammarström, 1996). Root surfaces covered by healthy cementum often appeared uneven, indicating earlier resorption defects that had only functionally but not anatomically been repaired. Root resorption lacunae in a reparatory phase containing new cementum have been described previously in control rat specimens (Brudvik and Rygh, 1993a). Apparently, rat molar roots normally have an uneven surface contour, possibly as a consequence of incidental resorption episodes during tooth eruption. In any case, roots with an uneven surface seemed to be readily resorbed, exposing dentinal tubules. The anatomic variation of the root surface contour may partly explain variations in individual susceptibility to root resorption during orthodontic tooth movement.

Small isolated resorption lacunae, as well as shallow resorption bays, were not uncommon in the control roots. Resorption defects on untreated or sham-operated teeth have been reported (Henry and Weinmann, 1951; Harry and Sims, 1982; Grevstad, 1987). Kvam (1972) has described small round cavities approximately 6 µm in diameter, which coincide with the present observations. Small isolated resorption bays near the root apex of human teeth which had recently acquired function, have been interpreted as sites of commencement of new cementum formation (Jones and Boyde, 1972). Small resorption pits have been considered to derive from a normal process, triggered by intermittent damage of the PDL and root surface at the margin of the alveolar bone crest (Hellsing and Hammarström, 1996).

#### *Experimental group*

The root surface was affected within one day following orthodontic force application. Degenerative changes in the PDL were accompanied by smoothing of the cementum surface, probably due to a breakdown of Sharpey's fibres. Similar changes in the root surface subjacent to coagulation necrosis have been attributed

to enzymes released from the mechanically damaged PDL (Brudvik and Rygh, 1994a; Hellsing and Hammarström, 1996). In some areas, presumably of moderate pressure, the thinning of the cementum could be attributed to superficial resorption which spreads readily. A few tissue remnants remained on the root despite the NaOCl extraction. Considering that PDL in pressure zones showed early signs of degeneration under LM, it could be hypothesized that remnants observed under SEM derive from necrotic (hyalinized) tissue (Reitan, 1951). Similar structures have previously been observed (Hellsing and Hammarström, 1996). Moreover, the continuity between periodontal fibrils and cementum has been found generally preserved in the compressed regions. In these areas of the PDL, fibrous elements were largely orientated parallel to the root surface (Rygh, 1973).

During the experimental period, the total area occupied by small isolated lacunae diminished, as these defects gradually fused with superficial resorption bays and deep lacunae. Their average diameter was also decreased on the last experimental day, as only the small lacunae at a distance from the main defect, probably excavated by relatively inactive cells, remained non-fused. Small isolated lacunae seem to be the effect of a single cell or even of a 'bite' corresponding to one ruffled border zone (Boyde and Jones, 1979). The present study indicated that mononuclear cells resembling macrophages and/or fibroblasts were associated with small isolated lacunae and superficial resorption.

Apart from clast cells, macrophages and fibroblasts may participate in tissue degradation on the pressure side (Kvam, 1970; Rygh, 1974; Lilja *et al.*, 1983; Brudvik and Rygh, 1993b). Fibroblasts have been shown to have phagocytose collagen fibrils inserted into the cementum as well as the substance of the cementum (Deporter and Brown, 1980; Deporter and Ten Cate, 1980). They are frequent in the physiological PDL and active on the root surface (Jäger *et al.*, 1993). Macrophages possess phagocytotic capacity for necrotic tissue, which is chemotactic for them. Mononuclear cells, presumably macrophages, have been shown to resorb osteoid (Rifkin *et al.*, 1980) as well as mineralized matrix (Rifkin *et al.*, 1979; Holtrop *et al.*, 1982; Wesselink *et al.*, 1986). In experimental periodontitis, they were shown to contain intracellular collagen fibrils (Rifkin and Heijl, 1979). Wedenberg and Lindskog (1986) have demonstrated the morphological transformation of a macrophage from inactive to active, colonizing different dental tissues, infected or uninfected. Inactive cells were spherical and unable to spread. On infected tissues they flattened out, developed broad cytoplasmic veils or long and slender filopod-like projections and were able to spread. Macrophage-like cells with membrane-ruffling, bleb-like projections and a peripheral smooth plasma membrane which spread along the cementum were seen in relation to shallow resorption lacunae on teeth with

non-vital PDL (Lindskog *et al.*, 1985). Endogenous resorption inhibitors may be responsible for the lack of macrophage spreading on non-mineralized pre-dentine (Lindskog and Hammarström, 1980). The results of the present study showed that small isolated lacunae may exist in control roots and that superficial resorption bays develop soon after force application. Additionally, a morphological continuity between the lacunae of these two types was often noticed. From these findings it may be hypothesized that relatively inactive cells of the mononuclear phagocyte system present in the PDL create the solitary small lacunae. Presumably, stimulation by local conditions, including substances released from necrotic tissue, may lead to their transformation into more active cells capable of amoeboid movement and a greater resorptive potential. The variation in cementum depth at the site of attack may reflect the different degree of activation. These cells may be responsible for superficial resorption bays, but are not capable of producing deep resorption defects.

It seems that superficial root resorption may be considered part of the mechanism of repair when the PDL is damaged, either as a consequence of periodontal disease and its treatment or during orthodontic tooth movement. The resorptive activity of fibroblasts has been proposed to be of central importance in the reorganization of the PDL during tooth movement (Ten Cate *et al.*, 1976). These cells have a key role in the maintenance of the PDL (Garant, 1976). During repair of the periodontal attachment apparatus, the root surface could also be resorbed by cells of the mononuclear phagocyte system. New Sharpey's fibres can then be included in the newly formed cementum and interdigitate with the existing matrix fibres (Stahl and Tarnow, 1985; Selvig *et al.*, 1988).

Deep lacunae occurred later in the experimental period, invariably within the field of superficial resorption bays. It seems that an initial superficial resorption process is essential for deeper lacunae to occur in a subsequent phase. It can be speculated that macrophage-like cells, which superficially resorb the root, may attract and activate clast cells with higher phagocytotic capacity, through the secretion of such substances as osteoclast activating factor and prostaglandins (Lindskog *et al.*, 1985). Clast cells may already be present close to the root, resorbing the necrotized PDL. In the absence of a protective barrier, they readily attack the exposed mineralized dental tissues (Rygh, 1977; Lindskog *et al.*, 1987). In areas of undamaged cementum the resorption continues as an undermining process, indicating the resistance to resorption of the healthy cementum surface.

### Conclusions

From the sequence of different types of lacuna observed during the initial stages of orthodontically induced

root resorption, it appears that different cell types with different resorptive potential are involved in the successive phases of the process. Isolated small and wide shallow lacunae, related to mononucleated macrophage-like cells, precede the appearance of deep lacunae excavated by multinucleated cells. This could indicate a functional relationship between them.

### Address for correspondence

Maria Mavragani  
Department of Dental Research  
Faculty of Dentistry  
University of Bergen  
Årstadveien 17  
N-5009 Bergen  
Norway

### Acknowledgements

The technical expertise and assistance of Mr Hugo Cato Olsen, Mr Odd Lundberg, Ms Rita Greiner-Simonsen, Ms Anita Koldingsnes, Ms Marit Simonsen, Ms Randi Sundfjord and Ms Siren Østvold are gratefully acknowledged. We wish to express our gratitude to Dr Olav Egil Bøe for statistical advice.

### References

- Barber A F, Sims M R 1981 Rapid maxillary expansion and external root resorption in man: a scanning electron microscope study. *American Journal of Orthodontics* 79: 630–652
- Boyde A, Jones S J 1968 Scanning electron microscopy of cementum and Sharpey fibre bone. *Zeitschrift für Zellforschung und Mikroskopische Anatomie* 92: 536–548
- Boyde A, Jones S J 1979 Estimation of the size of resorption lacunae in mammalian calcified tissues using SEM stereophotogrammetry. *Scanning Electron Microscopy* 2: 393–402
- Brudvik P, Rygh P 1993a The initial phase of orthodontic root resorption incident to local compression of the periodontal ligament. *European Journal of Orthodontics* 15: 249–263
- Brudvik P, Rygh P 1993b Non-clast cells start orthodontic root resorption in the periphery of hyalinized zones. *European Journal of Orthodontics* 15: 467–480
- Brudvik P, Rygh P 1994a Root resorption beneath the main hyalinized zone. *European Journal of Orthodontics* 16: 249–263
- Brudvik P, Rygh P 1994b Multi-nucleated cells remove the main hyalinized tissue and start resorption of adjacent root surfaces. *European Journal of Orthodontics* 16: 265–273
- Deporter D A, Brown D Y 1980 Fine structural observations on the mechanism of loss of attachment during experimental periodontal disease in the rat. *Journal of Periodontal Research* 15: 304–313
- Deporter D A, Ten Cate A R 1980 Collagen resorption by periodontal ligament fibroblasts at the hard tissue–ligament interfaces of the mouse periodontium. *Journal of Periodontology* 51: 429–432
- Garant P R 1976 Collagen resorption by fibroblasts. *Journal of Periodontology* 47: 380–390
- Grevstad H J 1987 Experimentally induced resorption cavities in rat molars. *Scandinavian Journal of Dental Research* 95: 428–440

- Harry M R, Sims M R 1982 Root resorption in bicuspid intrusion. A scanning electron microscope study. *Angle Orthodontist* 52: 235–258
- Helsing E, Hammarström L 1996 The hyaline zone and associated root surface changes in experimental orthodontics in rats: a light and scanning electron microscope study. *European Journal of Orthodontics* 18: 11–18
- Henry J L, Weinmann J P 1951 The pattern of resorption and repair of human cementum. *Journal of the American Dental Association* 42: 270–290
- Holtrop M E, Cox K A, Glowacki J 1982 Cells of the mononuclear phagocytic system resorb implanted bone matrix: a histologic and ultrastructural study. *Calcified Tissue International* 34: 488–494
- Jäger A, Radlanski R J, Götz W 1993 Demonstration of cells of the mononuclear phagocyte lineage in the periodontium following experimental tooth movement in the rat. An immunohistochemical study using monoclonal antibodies ED1 and ED2 on paraffin-embedded tissues. *Histochemistry* 100: 161–166
- Jones S J, Boyde A 1972 A study of human root cementum surfaces as prepared for and examined in the scanning electron microscope. *Zeitschrift für Zellforschung und Mikroskopische Anatomie* 130: 318–337
- Kvam E 1970 A study of the cell-free zone following experimental tooth movement in the rat. *Transactions of the European Orthodontic Society*, pp. 419–434
- Kvam E 1972 Cellular dynamics on the pressure side of the rat periodontium following experimental tooth movement. *Scandinavian Journal of Dental Research* 80: 369–383
- Kvam E 1973 Organic tissue characteristic on the pressure side of human premolars following tooth movement. *Angle Orthodontist* 43: 18–23
- Lilja E, Björnstedt T, Lindskog S 1983 Cellular enzyme activity associated with tissue degradation following orthodontic tooth movement in man. *Scandinavian Journal of Dental Research* 91: 381–390
- Lindskog S 1982 Formation of intermediate cementum. I: Early mineralization of aprismatic enamel and intermediate cementum in monkey. *Journal of Craniofacial Genetics and Developmental Biology* 2: 147–160
- Lindskog S, Hammarström L 1980 Evidence in favor of an anti-invasion factor in cementum or periodontal membrane of human teeth. *Scandinavian Journal of Dental Research* 88: 161–163
- Lindskog S, Lilja E 1984 Scanning electron microscopic study of orthodontically induced injuries to the periodontal membrane. *Scandinavian Journal of Dental Research* 92: 334–343
- Lindskog S, Pierce A M, Blomlöf L, Hammarström L 1985 The role of the necrotic periodontal membrane in cementum resorption and ankylosis. *Endodontics and Dental Traumatology* 1: 96–101
- Lindskog S, Blomlöf L, Hammarström L 1987 Cellular colonization of denuded root surfaces *in vivo*: cell morphology in dentin resorption and cementum repair. *Journal of Clinical Periodontology* 14: 390–395
- Reitan K 1951 The initial tissue reaction incident to orthodontic tooth movement. *Acta Odontologica Scandinavica* 9: supplement 6
- Reitan K 1974 Initial tissue behavior during apical root resorption. *Angle Orthodontist* 44: 68–82
- Reitan K, Kvam E 1971 Comparative behavior of human and animal tissue during experimental tooth movement. *Angle Orthodontist* 41: 1–14
- Rifkin B R, Heijl L 1979 The occurrence of mononuclear cells at sites of osteoclastic bone resorption in experimental periodontitis. *Journal of Periodontology* 50: 636–640
- Rifkin B R, Baker R L, Coleman S J 1979 An ultrastructural study of macrophage-mediated resorption of calcified tissue. *Cell and Tissue Research* 202: 125–132
- Rifkin B R, Baker R L, Somerman M J, Pointon S E, Coleman S J, William Y W 1980 Osteoid resorption by mononuclear cells *in vitro*. *Cell and Tissue Research* 210: 493–500
- Rygh P 1972 Ultrastructural vascular changes in pressure zones of rat molar periodontium incident to orthodontic movement. *Scandinavian Journal of Dental Research* 80: 307–321
- Rygh P 1973 Ultrastructural changes of the periodontal fibers and their attachment in rat molar periodontium incident to orthodontic tooth movement. *Scandinavian Journal of Dental Research* 81: 467–480
- Rygh P 1974 Elimination of hyalinized periodontal tissues associated with orthodontic tooth movement. *Scandinavian Journal of Dental Research* 82: 57–73
- Rygh P 1977 Orthodontic root resorption studied by electron microscopy. *Angle Orthodontist* 47: 1–16
- Selvig K A 1964 An ultrastructural study of cementum formation. *Acta Odontologica Scandinavica* 22: 105–120
- Selvig K A, Bogle G, Claffey N M 1988 Collagen linkage in periodontal connective tissue reattachment. An ultrastructural study in beagle dogs. *Journal of Periodontology* 59: 758–768
- Stahl S S, Tarnow D 1985 Root resorption leading to linkage of dentinal collagen and gingival fibers? A case report. *Journal of Clinical Periodontology* 12: 399–404
- Stephens M A 1974 EDF statistics for goodness of fit and some comparisons. *Journal of the American Statistical Association* 69: 730–737
- Ten Cate A R, Deporter D A, Freeman E 1976 The role of fibroblasts in the remodeling of periodontal ligament during physiologic tooth movement. *American Journal of Orthodontics* 69: 155–168
- Warshawsky H, Moore G A 1967 A technique for the fixation and decalcification of rat incisors for electron microscopy. *Journal of Histochemistry and Cytochemistry* 15: 542–549
- Wedenberg C, Lindskog S 1986 Macrophage colonization of infected and non-infected dental tissues *in vitro*. *Scandinavian Journal of Dental Research* 94: 311–319
- Wesselink P R, Beertsen W, Everts V 1986 Resorption of the mouse incisor after the application of cold to the periodontal attachment apparatus. *Calcified Tissue International* 39: 11–21

Copyright of European Journal of Orthodontics is the property of Oxford University Press / UK and its content may not be copied or emailed to multiple sites or posted to a listserv without the copyright holder's express written permission. However, users may print, download, or email articles for individual use.